Available online at www.sciencedirect.com

ScienceDirect

Journal of Computational and Applied Mathematics 207 (2007) 273–290

JOURNAL OF COMPUTATIONAL AND APPLIED MATHEMATICS

www.elsevier.com/locate/cam

On the use of Hadamard expansions in hyperasymptotic evaluation of Laplace-type integrals—III: Clusters of saddle points

R.B. Paris*

Division of Mathematical Sciences, University of Abertay Dundee, Dundee DD1 1HG, UK

Dedicated to Nico M. Temme on the occasion of his 65th birthday

Abstract

It is shown how the recently developed Hadamard expansion procedure can be applied to the hyperasymptotic evaluation of Laplace-type integrals containing a large variable when the phase function has a cluster of close-lying saddle points. The modification to this procedure that is required when the saddles in the cluster coalesce to form a single higher-order saddle is discussed. An example is also considered in which there is both a coalescence of saddles and a Stokes phenomenon as the phase of the large variable is allowed to vary. Numerical examples are given to illustrate the accuracy that can be obtained with this new procedure.

MSC: 30E15; 30E20; 41A60

Keywords: Asymptotics; Hyperasymptotics; Hadamard expansions; Laplace-type integrals; Clusters of saddles

1. Introduction

The theory of uniform asymptotic expansions of functions defined by integrals has undergone a steady development since the seminal paper of Chester et al. [2] in 1957 on Laplace-type integrals containing a pair of coalescing saddle points. Since that time, techniques for coping with a wide variety of saddle-point uniformity problems have appeared, including means for handling a saddle point near a pole, a saddle point near an endpoint of an integration contour and three or more saddle points coalescing to a single point. Probably the most elaborate of the saddle-point coalescence problems was analysed by Berry and Howls [1] and applies to Laplace-type integrals with several saddles, some of which can coalesce as a parameter is varied. The desire for high-precision asymptotics has led to expansions that capitalise on 'resurgence' (the re-expression of the remainder term in a steepest descent approximation in terms of steepest descent expansions at other saddle points) and multiple scattering amongst other saddle points (a by-product of resurgence).

The process can be very involved and, to a nonpractitioner of high-precision or uniform asymptotics, the nature of such recent investigations might appear to be rather arcane. Yet, applications in natural science *can* involve clusters of saddle points undergoing a variety of behaviours, with diffraction theory being a rich source of such problems. The well-known Pearcey integral contains two parameters that when varied can result in both coalescence of saddles and

* Tel.: +44 138 2308618; fax: +44 138 2308627.
E-mail address: r.paris@abertay.ac.uk.

0377-0427/$ - see front matter © 2006 Elsevier B.V. All rights reserved.
doi:10.1016/j.cam.2006.10.016

the Stokes phenomenon [13,11, Section 8.3]. Another example is the recent paper by Kazakov [5], which involved a Laplace-type integral with six saddle points depending on parameters that can undergo coalescence as the parameters vary.

We present here a means of systematic construction of high-precision approximations of such integrals with complicated saddle-point structure, which retain their utility as parameters vary. Our approach will use the recently developed theory of Hadamard expansions, and for completeness of exposition, a brief overview of this theory is supplied with references to more detailed accounts in the literature. We remark that numerical schemes involving related expansions have recently been proposed for the numerical evaluation of the Kummer functions in [6,7] and for the exponential integral in [3].

The application of this expansion procedure to the evaluation of Laplace-type integrals of the form

$$J(z)=\int_C \mathrm{e}^{-z\psi(t)} f(t)\,\mathrm{d}t \quad (|z|\to\infty), \tag{1.1}$$

where the phase function $\psi(t)$ possesses saddle points (given by the points where $\psi'(t)=0$) has been elaborated in [8,9]. The integration path C in the complex t-plane may be finite or infinite and is supposed to coincide with paths of steepest descent through one or more saddles. The function $f(t)$ is assumed to be analytic on and near C. In the case when C passes through a single saddle point t_s, it was shown by appropriate subdivision of the integration path that the integral $J(z)$ could be expressed *exactly* as an expansion involving a sequence of exponential levels of increasing subdominance in the form

$$J(z)=\mathrm{e}^{-z\psi(t_s)}\sum_n \mathrm{e}^{-\Omega_n|z|}S_n(z).$$

The number of levels n may be finite or infinite depending on whether C is finite or infinite. Each exponential factor in the sum is multiplied by a Hadamard series $S_n(z)$ of the form

$$S_n(z)=\sum_{k=0}^{\infty}\frac{c_{kn}}{(\omega_n z)^{\alpha_n k+\beta_n}}P(\alpha_n k+\beta_n,\omega_n|z|), \tag{1.2}$$

where c_{kn} are coefficients that result from appropriate series expansion of the integrand and $P(a,x)$ denotes the normalised incomplete gamma function

$$P(a,x)=\frac{\gamma(a,x)}{\Gamma(a)}=\frac{1}{\Gamma(a)}\int_0^x \mathrm{e}^{-t}t^{a-1}\,\mathrm{d}t \quad (|\arg x|<\pi,\ \mathrm{Re}(a)>0)=\frac{x^a\mathrm{e}^{-x}}{\Gamma(1+a)}{}_1F_1(1;1+a;x). \tag{1.3}$$

The quantities ω_n are specified by the radii of convergence in the expansion of the integrand of (1.1) along the path C, which in turn are controlled by the saddle-point structure of $\psi(t)$ and the singularities of $f(t)$. The exponential levels Ω_n are given by $\Omega_n=\sum_{r=0}^{n-1}\omega_r$ $(n\geqslant 1)$, with $\Omega_0=0$, and consequently form a nonnegative, monotonically increasing sequence. The α_n and β_n are positive parameters that depend on the order of the saddle point t_s and on whether t_s is an endpoint or an internal point of C. The function $P(a,x)$ exhibits a 'cut-off' behaviour [8] in a for large positive variables, with the consequence that the Hadamard series $S_n(z)$ consist of terms of a Poincaré-type asymptotic expansion $\sum c_{kn}(\omega_n z)^{-\alpha_n k-\beta_n}$, with coefficients c_{kn} and asymptotic scale $(\omega_n z)^{\alpha_n}$, 'smoothed' by the factor $P(a,x)$. The presence of this smoothing factor (in combination with a possible restriction on the parameters β_n) then ensures that each series $S_n(z)$ is *absolutely convergent*, rather than asymptotic. The terms in $S_n(z)$ therefore behave approximately like an asymptotic series down to its optimal truncation point, followed (usually) by a much slower decay past this point.

In [8], it was shown that each Hadamard series can be modified by a simple rearrangement of the terms in the tail of the series to produce expansions with a rapid decay when $|z|$ is large. By this means, it is possible to represent $J(z)$ by a convergent sum of absolutely convergent series, each associated with an increasingly subdominant exponential level. For large $|z|$, the terms in each modified series then behave like those of an asymptotic expansion down to the optimal truncation point but *continue to decay at a comparable rate past this point*. Such an expansion procedure provides a computationally attractive method of hyperasymptotic evaluation and in the process 'exactifies' the classical asymptotic procedure known as the method of steepest descents [10].

The structure of the paper is as follows. In Section 2, we describe the procedure for the simple case when the path C in (1.1) commences at a particular saddle and passes to infinity along a steepest descent curve in an appropriate direction. In the remainder of the paper we shall discuss three specific examples of Laplace-type integrals that can be regarded as illustrative of the methodology we employ and that highlight the various complications that can arise when dealing with clusters of saddle points. Numerical results are given in each case to illustrate the accuracy achievable with this procedure.

2. The Hadamard expansion of $J(z)$ in a simple case

To explain the development of Hadamard expansions for the integral $J(z)$ in (1.1), let us consider the situation where the integration path C commences at a particular saddle t_s, say, and passes to infinity along a steepest descent path, defined by

$$\mathrm{Im}(\mathrm{e}^{\mathrm{i}\theta}\{\psi(t)-\psi(t_s)\})=0 \quad (\theta=\arg z),$$

in an appropriate direction; see Fig. 1. We shall assume in what follows that the particular path of steepest descent chosen does not connect with another saddle thereby removing from our deliberations at this stage the possibility of a Stokes phenomenon.

With the change of variable $u=\mathrm{e}^{\mathrm{i}\theta}\{\psi(t)-\psi(t_s)\}$ in (1.1) we find

$$J(z)=\mathrm{e}^{-z\psi(t_s)}\int_0^\infty \mathrm{e}^{-|z|u} f(t)\frac{\mathrm{d}t}{\mathrm{d}u}\,\mathrm{d}u; \tag{2.1}$$

in general, the integrand will possess an integrable singularity at $u=0$. The integration path in the u-plane (the so-called Borel plane) is now subdivided into a series of finite segments of length ω_n ($n=0,1,2,\ldots$) with left-hand endpoints $u=\Omega_n$, where $\Omega_0=0$ and

$$\Omega_n=\sum_{r=0}^{n-1}\omega_r \quad (n\geqslant 1). \tag{2.2}$$

The sequence of points $u=\Omega_n$ corresponds to the sequence t_n situated on the steepest descent path through t_s (with $t_0\equiv t_s$), where the t_n are determined by solution of $\Omega_n=\mathrm{e}^{\mathrm{i}\theta}\{\psi(t_n)-\psi(t_s)\}$; see Fig. 1. The above definitions of u and Ω_n then lead to

$$\psi(t)-\psi(t_n)=(u-\Omega_n)\mathrm{e}^{-\mathrm{i}\theta}=\omega_n v\mathrm{e}^{-\mathrm{i}\theta}, \tag{2.3}$$

where the scaled variable v is defined by $u=\Omega_n+\omega_n v$, $0\leqslant v\leqslant 1$.

Inversion of (2.3) yields

$$t-t_n=\sum_{k=0}^{\infty} b_{kn}(v\mathrm{e}^{-\mathrm{i}\theta})^{(k+1)\mu_n}, \quad \mu_n=\begin{cases}\frac{1}{2} & (n=0),\\ 1 & (n\geqslant 1),\end{cases} \tag{2.4}$$

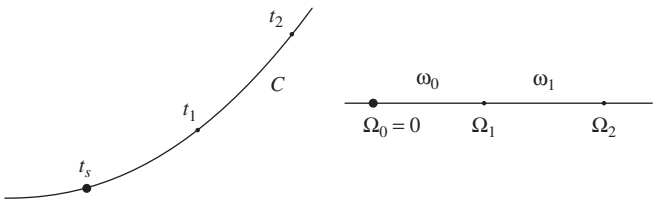

Fig. 1. The steepest descent path through the saddle t_s showing the points $t_1, t_2, \ldots$ and the corresponding points Ω_n along the u-axis.

where, in particular, $b_{00} = (2\omega_0/\psi''(t_s))^{1/2}$ and $b_{0n} = \omega_n/\psi'(t_n)$ $(n \geqslant 1)$. Then we can write the series expansion of $f(t)\,\mathrm{d}t/\mathrm{d}v$ about the sequence of points t_n in the form

$$f(t)\frac{\mathrm{d}t}{\mathrm{d}v} = \mathrm{e}^{-\mathrm{i}\theta}\sum_{k=0}^{\infty}\frac{c_{kn}}{\Gamma((k+1)\mu_n)}(v\mathrm{e}^{-\mathrm{i}\theta})^{(k+1)\mu_n-1}, \tag{2.5}$$

where the c_{kn} are coefficients with

$$c_{0n} = \Gamma(1+\mu_n)b_{0n}f(t_n) \quad (n = 0, 1, 2, \ldots).$$

If the interval length ω_n is chosen to be the radius of convergence of the expansion (2.5) about t_n then each series converges in $|v| < 1$. The precise values of ω_n and Ω_n then depend on the location of other saddle points of $\psi(t)$ and on the singularity structure of $f(t)$ [8].

The contribution to $J(z)$ from the nth interval $\Omega_n \leqslant u \leqslant \Omega_{n+1}$ (that is, between the points t_n and t_{n+1} on the steepest descent path) is given by

$$\begin{aligned}\mathrm{e}^{-z\psi(t_s)-\Omega_n|z|}\int_0^1 \mathrm{e}^{-|z|\omega_n v}f(t)\frac{\mathrm{d}t}{\mathrm{d}v}\,\mathrm{d}v &= \mathrm{e}^{-z\psi(t_s)-\Omega_n|z|}\sum_{k=0}^{\infty}\frac{c_{kn}\mathrm{e}^{-\mathrm{i}\theta}}{\Gamma((k+1)\mu_n)}\int_0^1 \mathrm{e}^{-|z|\omega_n v}(v\mathrm{e}^{-\mathrm{i}\theta})^{(k+1)\mu_n-1}\,\mathrm{d}v\\ &= \mathrm{e}^{-z\psi(t_s)-\Omega_n|z|}S_n(z),\end{aligned} \tag{2.6}$$

where $S_n(z)$ is the Hadamard series at level n defined in (1.2) with $\alpha_n = \beta_n = \mu_n$, namely

$$S_n(z) = \sum_{k=0}^{\infty}\frac{c_{kn}}{(\omega_n z)^{(k+1)\mu_n}}\,P((k+1)\mu_n, \omega_n|z|). \tag{2.7}$$

The Hadamard expansion of the integral $J(z)$ in (1.1), when C is taken along a semi-infinite steepest descent path commencing at the saddle t_s, then takes the form

$$J(z) = \mathrm{e}^{-z\psi(t_s)}\sum_{n=0}^{\infty}\mathrm{e}^{-\Omega_n|z|}S_n(z), \tag{2.8}$$

where each Hadamard series $S_n(z)$ is associated with the decreasing exponential level $\exp(-\Omega_n|z|)$. The modification of the argument leading to (2.8) when the path C in (1.1) is doubly infinite is straightforward and consists mainly of a cancellation of the odd terms in the zeroth-level series $S_0(z)$ on either side of the saddle to yield a series of the type (1.2) with $\alpha_0 = 1$ and $\beta_0 = \frac{1}{2}$; see [8,10].

The values of the exponential levels Ω_n are controlled by the intervals ω_n through (2.2), which are in turn determined either by the saddle-point structure of $\psi(t)$ in the t-plane or by the possible presence of singularities of the amplitude function $f(t)$. We shall assume throughout in this paper that any singularities of $f(t)$ are remote with respect to the cluster and so are not effective in the determination of the convergence intervals.[1] Thus, when expanding about the saddle t_s, the zeroth interval ω_0 is determined by the nearest saddle point. This value of ω_0 then fixes the value of Ω_1 (and hence t_1 in the t-plane). The value of ω_1 for the next interval is determined either by the saddle t_s or by the nearest of the distant saddles. Provided the other saddles are sufficiently distant, the convergence intervals ω_n for $n \geqslant 1$ will, generally speaking, be controlled by the saddle t_s and so will increase progressively with n. This represents the straightforward situation in which the Hadamard expansion (2.8) for large $|z|$ consists of well-separated exponential levels. When we are dealing with clusters of saddle points, however, one or more of the distant saddles can start to coalesce with the saddle t_s as some parameter a, say, contained in $\psi(t)$ approaches a critical value a_0. Then it is clear that the zeroth interval ω_0 shrinks to zero as $a \to a_0$. The remaining intervals ω_n depend on ω_0 and so will similarlyshrink to zero, with the result that all the levels $\Omega_n \to 0$ in this limit. In this situation the Hadamard expansion (2.8) suffers from a progressive loss of exponential separation between the different levels.

[1] The treatment of the case when singularities of $f(t)$ enter the cluster or approach either the saddle t_s or the integration path C will be discussed in the final paper of this series.

To overcome this problem we proceed as described in [10,12]. Instead of expanding about the saddle t_s, we expand about a point t_1 on the steepest descent path through this saddle *which is chosen independently of the proximity of the nearby coalescing saddle*. Then, provided the discs of convergence of the expansion (2.5) about t_1 and the subsequent points t_n ($n \geqslant 2$) on this path are controlled by the saddle t_s (and not by one of the coalescing saddles or by a singularity of $f(t)$), the value[2] of the zeroth interval ω_0 is accordingly

$$\omega_0 = \Omega_1 = \mathrm{e}^{\mathrm{i}\theta}\{\psi(t_1) - \psi(t_s)\} \tag{2.9}$$

with the other intervals determined by

$$\omega_n = \Omega_n = 2^{n-1}\omega_0 \quad (n \geqslant 1). \tag{2.10}$$

(When the inversion of (2.3) is not controlled by the saddle t_s, but by one of the neighbouring saddles, then a further modification is necessary; see the end of Section 3.1 for an example.) With $u = \Omega_1 + \omega_0 v$, where now $-1 \leqslant v \leqslant 0$, the contribution from the zeroth interval between t_s and t_1 becomes

$$\mathrm{e}^{-z\psi(t_s)} \int_0^{\Omega_1} \mathrm{e}^{-|z|u} f(t) \frac{\mathrm{d}t}{\mathrm{d}u}\, \mathrm{d}u = \mathrm{e}^{-z\psi(t_s)-\omega_0|z|} \int_{-1}^{0} \mathrm{e}^{-|z|\omega_0 v} f(t) \frac{\mathrm{d}t}{\mathrm{d}v}\, \mathrm{d}v = \mathrm{e}^{-z\psi(t_s)} \mathbf{S}_0(z),$$

where we have defined the new zeroth-level Hadamard series

$$\mathbf{S}_0(z) = -\mathrm{e}^{-\omega_0|z|} \sum_{k=0}^{\infty} \frac{c_{k1}}{(\omega_0 z)^{k+1}} P(k+1, -\omega_0|z|) \tag{2.11}$$

and the coefficients c_{k1} are specified by (2.5) with $n = 1$.

The contributions from the remaining intervals with $n \geqslant 1$ are the same as those in (2.8) but based on the new sequence of points $t_1, t_2, \ldots$. Then an alternative form for the Hadamard expansion of the integral $J(z)$ suitable for the case of coalescing saddles is given by

$$J(z) = \mathrm{e}^{-z\psi(t_s)} \sum_{n=0}^{\infty} \mathrm{e}^{-\Omega_n|z|} \mathbf{S}_n(z), \tag{2.12}$$

where, for convenience in presentation, we have set $\mathbf{S}_n(z) = S_n(z)$ for $n \geqslant 1$. We remark that there is a certain flexibility in the choice of the point t_1 (and hence of ω_0) but that this choice reflects ultimately on the rate of convergence of the series $\mathbf{S}_0(z)$: the larger the value of ω_0, the slower the rate of convergence [10]. Consequently, the choice of ω_0 is a compromise between the desired exponential separation of the different levels in (2.12) and the number of terms to be computed in the zeroth-level tail.

The convergence and the computation of the Hadamard series $S_n(z)$ and $\mathbf{S}_0(z)$ have been discussed in detail in [8–10]. For large values of $|z|$, it was shown that if each Hadamard series is truncated after M_n terms (to produce the finite main sum) the slowly convergent tail of the series could be converted, for suitable choice of truncation index M_n, into a tail that converges roughly as rapidly as the asymptotic-like finite main sum. We write

$$\mathscr{S}_n(z) = \pm A(z) \sum_{k=0}^{M_n-1} \frac{c_{km}}{(\omega_n z)^{\alpha_n k+\beta_n}} P(\alpha_n k + \beta_n, \pm\omega_n|z|) + \mathscr{T}_n(M_n; z), \tag{2.13}$$

where $\mathscr{S}_n(z)$ and $\mathscr{T}_n$ refer to either $S_n(z)$ in (2.7) and its tail T_n ($n \geqslant 0$), or to $\mathbf{S}_0(z)$ in (2.11) and its tail $\mathbf{T}_0$. In the case of $S_n(z)$, we have $A(z) = 1$, $m = n$, $\alpha_n = \beta_n = \mu_n$ with the upper sign being chosen and in the case of $\mathbf{S}_0(z)$, we have $A(z) = \mathrm{e}^{-\omega_0|z|}$, $m = 1$, $\alpha_0 = \beta_0 = 1$ with the lower sign being chosen. The tail $\mathscr{T}_n(M_n; z)$ can be rearranged into a rapidly convergent form by replacement of the normalised incomplete gamma function by its hypergeometric function

[2] In practice, it is easier to choose ω_0 and thence to determine t_1 by solution of (2.3) with $n = 1$.

representation in (1.3), followed by reversal of the order of summation in the resulting double sum, to produce

$$\mathscr{T}_n(M_n;z) = \pm A(z)\sum_{k=M_n}^{\infty}\frac{c_{km}}{(\omega_n z)^{\alpha_n k+\beta_n}}P(\alpha_n k+\beta_n,\pm\omega_n|z|)$$

$$= A(z)\mathrm{e}^{\mp\omega_n|z|}\sum_{r=0}^{\infty}\sigma_{r,n}(\pm\chi_n)^r, \quad \chi_n=\omega_n|z|/M_n. \tag{2.14}$$

The coefficients $\sigma_{r,n}\equiv\sigma_{r,n}(M_n)$ are defined by

$$\sigma_{r,n} = \pm M_n^r\sum_{k=M_n}^{\infty}\frac{c_{km}(\pm\mathrm{e}^{-\mathrm{i}\theta})^{\alpha_n k+\beta_n}}{(\alpha_n k+\beta_n+r)!} = M_n^r\left\{s_n\mp\sum_{k=0}^{M_n-1}\frac{c_{km}(\pm\mathrm{e}^{-\mathrm{i}\theta})^{\alpha_n k+\beta_n}}{(\alpha_n k+\beta_n+r)!}\right\}, \tag{2.15}$$

where s_n represents the sum over $0\leqslant k\leqslant\infty$. In [9,10], it is shown that s_n can be expressed in terms of the integrals

$$s_n = \begin{cases}\dfrac{1}{r!}\displaystyle\int_{t_n}^{t_{n+1}}(1-v_n)^r f(t)\,\mathrm{d}t & \text{for } S_n(z)\\ \quad (n=0,1,2,\ldots), & \\ \dfrac{1}{r!}\displaystyle\int_{t_0}^{t_1} v_0^r f(t)\,\mathrm{d}t & \text{for } \mathbf{S}_0(z),\end{cases} \tag{2.16}$$

where $t_0\equiv t_s$ and, from (2.3), the variable $v_n\equiv v_n(t)$ is given by

$$v_n = \frac{\psi(t)-\psi(t_n)}{\omega_n\mathrm{e}^{-\mathrm{i}\theta}} \quad (n=0,1,2,\ldots). \tag{2.17}$$

We observe that, for $S_n(z)$, the tail T_n is multiplied by the exponentially small factor $\exp(-\omega_n|z|)$, since $A(z)=1$, thereby indicating the level at which the tail contributes. In the case of $\mathbf{S}_0(z)$, however, this exponential factor is not present in the tail $\mathbf{T}_0$.

This concludes our summary of the Hadamard expansion of integrals of the type $J(z)$ when the integration path C commences at a saddle t_s and follows a steepest descent path to infinity without encountering another saddle. The interested reader can find fuller details in the references cited above. We shall now exploit these results in a series of examples involving clusters of saddle points.

3. An example involving a cluster of two saddles

Our first example is the function defined by the integral

$$I(z;a) = \int_C \mathrm{e}^{-z\psi(t)}\,\mathrm{d}t, \quad \psi(t) = \tfrac{1}{4}t^4-\tfrac{2}{3}t^3+\tfrac{1}{2}(1-a)t^2, \tag{3.1}$$

where $f(t)=1$ and $z=x\mathrm{e}^{\mathrm{i}\theta}$, with $x>0$ and $\theta=\arg z$, which will be used to illustrate the Hadamard expansion procedure in the presence of two very different asymptotic phenomena: coalescence and the Stokes phenomenon. This integral was used as an example of hyperasymptotic expansion in [1, Section 4]. The integration path C is chosen to run from $-\infty$ to $+\infty\mathrm{i}$, thereby defining $I(z;a)$ in the sector $|\arg z|\leqslant\frac{1}{2}\pi$; extension beyond this sector can be accomplished by appropriate rotation of the contour. The quantity a is the coalescence parameter (here assumed to be real) and the integrand is characterised by a remote saddle at $t=0$ and a cluster of two saddles at $1\pm a^{1/2}$ that coalesce to form a double saddle when $a=0$. For $a>0$, the saddles in the cluster are situated on the real axis and are labelled $t_{sj}=1\mp a^{1/2}$ ($j=1,2$), respectively; for $a<0$, they move into the complex t-plane as a complex conjugate pair and in this case $t_{sj}=1\pm\mathrm{i}(-a)^{1/2}$.

Typical paths of steepest descent connecting the valleys containing $-\infty$ and $\infty\mathrm{i}$ are illustrated in Fig. 2 for different θ and small $|a|$. As the phase of z is allowed to vary, it is found that a Stokes phenomenon takes place on $\theta=0$

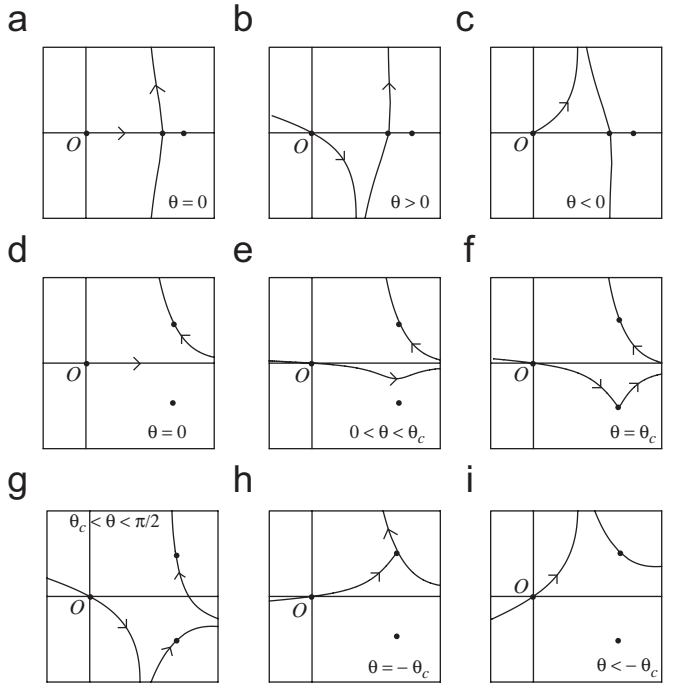

Fig. 2. The steepest descent paths in the t-plane for different values of θ: (a)–(c) when $0 < a < 1$ and (d)–(i) when $-a_* < a < 0$. The heavy dots are the saddle points and the arrows denote the direction of integration from O. Only the relevant paths are shown.

(when $0 < a < 1$) and on portions of the curves[3] $\theta = \pm\theta_c(a)$ (when $a < 0$), where

$$\tan\theta_c(a) = \frac{\frac{8}{3}(-a)^{3/2}}{\frac{1}{3} - 2a - a^2}. \tag{3.2}$$

These Stokes curves correspond to the steepest descent path through the origin connecting with the saddle t_{s1} in the cluster when $0 < a < 1$ and either t_{s1} (lower curve) or t_{s2} (upper curve) when $a < 0$. In addition, there is also a Stokes phenomenon when $\theta = \frac{1}{2}\pi$ and $a < 0$ resulting from the connection of the saddles t_{s1} and t_{s2}. In the a, θ-plane, this latter curve and the Stokes curve $\theta_c(a)$ intersect when $a = -a_*$, where $a_* = 1 + \frac{2}{\sqrt{3}}$; to the left of this point, both of these Stokes curves become inactive [4]. The Stokes curves for $a < 1$ are illustrated in Fig. 3 where the numbers of contributory saddles for the contour C in (3.1) are also indicated.

3.1. The case $0 \leqslant a < 1$

We first discuss the case $0 \leqslant a < 1$ which is associated with a Stokes phenomenon on $\theta = 0$. Our principal interest will concern the case $\theta > -\varepsilon$, where ε denotes a small positive angle, since from Fig. 2(c) the steepest descent path corresponding to $\theta < -\varepsilon$ consists of the single path through the remote saddle at $t = 0$ which does not pass close to the cluster. Evaluation of the integral (3.1) in this latter case is straightforward and is discussed in [8]. For simplicity in presentation, we shall now modify the path C by excluding the contribution from the path situated in the left half-plane, since its evaluation likewise presents no special difficulty. Consequently, we shall henceforth take the path C to commence at the saddle $t = 0$ and to pass to infinity in the valley containing the ray $\arg t = \frac{1}{2}\pi - \frac{1}{4}\theta$, thereby concentrating our attention on the two types of asymptotic phenomenon (coalescence and the Stokes phenomenon) associated with (3.1).

[3] This corresponds to the curves on which $\mathrm{Im}\{e^{i\theta}\psi(t_{sj})\} = 0$, $j = 1, 2$.

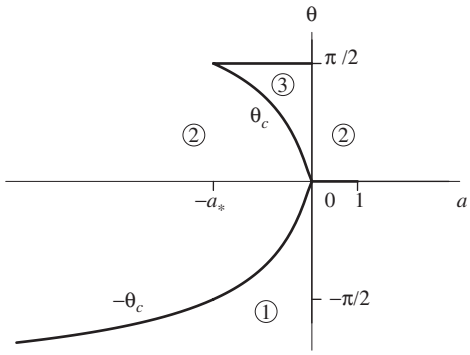

Fig. 3. The Stokes curves (bold) for $I(z;a)$ in the a, θ-plane when the coalescence parameter $a<1$. The encircled numbers denote the number of contributory saddles.

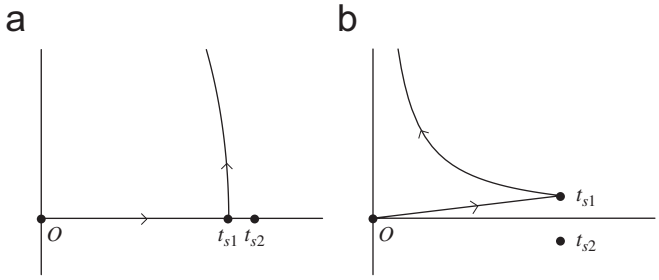

Fig. 4. The modified integration path when (a) $0<a<1$ and (b) $a<0$.

Following the discussion in [9] and in Section 2, the normal approach to take when z is complex would be to represent $I(z;a)$ as a sum of steepest descent contours and thence proceed to construct Hadamard expansions associated with each contour integral. This process results in series whose associated incomplete gamma functions have arguments that are positive (compare (2.7) and (2.8)) which produces the most rapid rate of convergence for the expansion. If we are willing to accept slightly less rapidly converging series, then much of the computational effort of the above path decomposition can be avoided by taking as our modified integration path that illustrated in Fig. 4(a). This consists of replacing C by the segment of the real axis $[0, t_{s1}]$ (*independently of the value of* θ) followed by the upper half of the steepest descent path through the saddle t_{s1} (which, of course, is θ-dependent). In this manner, we can cover the three situations depicted in Fig. 2 (a)–(c) when $0<a<1$ with a single path decomposition which, as we shall show below, is valid for $|\theta|\leqslant\frac{1}{2}\pi$. We shall label the contributions to $I(z;a)$ from these two paths by I_1 and I_2, respectively.[4]

From (2.3), the change of variable $u=\psi(t)-\psi(0)=\omega_0 v$, where $\omega_0=\psi(t_{s1})-\psi(0)$, yields the contribution from the interval $[0, t_{s1}]$ in the form

$$I_1\equiv\int_0^{t_{s1}}\mathrm{e}^{-z\psi(t)}\,\mathrm{d}t=\int_0^1\mathrm{e}^{-z\omega_0 v}\frac{\mathrm{d}t}{\mathrm{d}v}\,\mathrm{d}v.$$

A procedure identical to that employed in obtaining (2.7)—with θ effectively set equal to zero in (2.3) and $|z|$ replaced by z—shows that I_1 has the Hadamard expansion

$$I_1=\sum_{k=0}^{\infty}\frac{c_{k0}}{(\omega_0 z)^{(k+1)/2}}P\left(\tfrac{1}{2}k+\tfrac{1}{2},\omega_0 z\right). \tag{3.3}$$

[4] In order not to overburden the notation, we shall not distinguish between the coefficients c_{kn}, nor the quantities ω_n and Ω_n, resulting from the different integration paths. It is understood that their precise values will be different for the integrals I_1 and I_2.

The coefficients c_{k0} result from the inversion of the above change of variable which, from (2.4) with $n=0$, takes the form

$$\frac{\mathrm{d}t}{\mathrm{d}v}=\sum_{k=0}^{\infty}\frac{c_{k0}}{\Gamma(\frac{1}{2}k+\frac{1}{2})}v^{(k-1)/2}\quad(|v|<1)$$

with $c_{00}=\{\pi\omega_0/(2(1-a))\}^{1/2}$. This expansion converges in the unit disc $|v|<1$ since the inversion about the saddle $t=0$ is controlled by the saddle t_{s1}. We note that, because the path $[0,t_{s1}]$ is not a steepest descent path (except when $\theta=0$), the argument of the normalised incomplete gamma functions in (3.3) is complex. The modification of the expansion (3.3) into a finite main sum and a rapidly convergent tail follows the procedure detailed in Section 2 with obvious modifications, and we find

$$I_1=\sum_{k=0}^{M_0-1}\frac{c_{k0}}{(\omega_0 z)^{(k+1)/2}}P\left(\tfrac{1}{2}k+\tfrac{1}{2},\omega_0 z\right)+\mathrm{e}^{-\omega_0 z}\sum_{r=0}^{\infty}\sigma_{r,0}\chi_0^r, \tag{3.4}$$

with $\chi_0=\omega_0 z/M_0$. The coefficients $\sigma_{r,0}$ are specified by

$$\sigma_{r,0}=M_0^r\left\{\frac{1}{r!}\int_0^{t_{s1}}(1-v_0)^r\,\mathrm{d}t-\sum_{k=0}^{M_0-1}\frac{c_{k0}}{\Gamma(\frac{1}{2}k+r+\frac{3}{2})}\right\},$$

where, since $\psi(0)=0$, we have $v_0=\psi(t)/\omega_0$.

The normal procedure for dealing with the contribution I_2 from the steepest descent path through the saddle t_{s1} follows a decomposition of the steepest descent path into segments with endpoints at t_n $(n\geqslant 1)$, which leads to an expansion of type (2.8). As pointed out in Section 2, however, in the small a-limit the saddle t_{s2} will control the disc of convergence of the inversion about t_{s1}. This has the consequence that all the convergence intervals ω_n shrink to zero as $a\to 0$, which in turn results in a progressive loss of exponential separation between the different levels in the expansion (2.8). To overcome this difficulty, we employ the alternative expansion (2.12), which in this case becomes

$$I_2=\mathrm{e}^{-z\psi(t_{s1})}\sum_{n=0}^{\infty}\mathrm{e}^{-\Omega_n|z|}\mathbf{S}_n(z), \tag{3.5}$$

where, from (2.7) and (2.11),

$$\mathbf{S}_n(z)=A(z)\sum_{k=0}^{\infty}\frac{c_{km}}{(\omega_n z)^{k+1}}P(k+1,(-)^{\delta}\omega_n|z|),$$

with

$$A(z)=\begin{cases}-\mathrm{e}^{-\omega_0|z|},\\ 1,\end{cases}\qquad \delta=\begin{cases}1 & (n=0),\\ 0 & (n\geqslant 1)\end{cases}$$

and $m=n+\delta$. The quantities ω_n, Ω_n are defined in (2.9) and (2.10) and the coefficients c_{kn} $(n\geqslant 1)$ are specified by (2.4).

The choice of the endpoint t_1 on the steepest descent path through t_{s1}, and hence ω_0 by (2.9), can be made with a certain amount of flexibility; see Section 2. Then the integral $I(z;a)$ is given by

$$I(z;a)=I_1+I_2. \tag{3.6}$$

To illustrate, we consider $a=10^{-4}$ so that the saddles in the cluster are situated at $t_{s1}=0.99$ and $t_{s2}=1.01$. We take $|z|=20$ and compute the expansions in (3.3) and (3.5) for different θ in the range $|\theta|\leqslant\frac{1}{2}\pi$. The Hadamard series in (3.3) and (3.5) are appropriately truncated (so that the variable $|\chi_n|<1$), with their corresponding modified tails computed from (2.14) to (2.16). The points t_n on the steepest descent path though t_{s1} are obtained from (2.9) and (2.10) with the value of $\omega_0=0.75$. The coefficients c_{kn} are determined by the numerical inversion routine in *Mathematica*. The tails are truncated after N_n terms commensurate with the level of precision required.

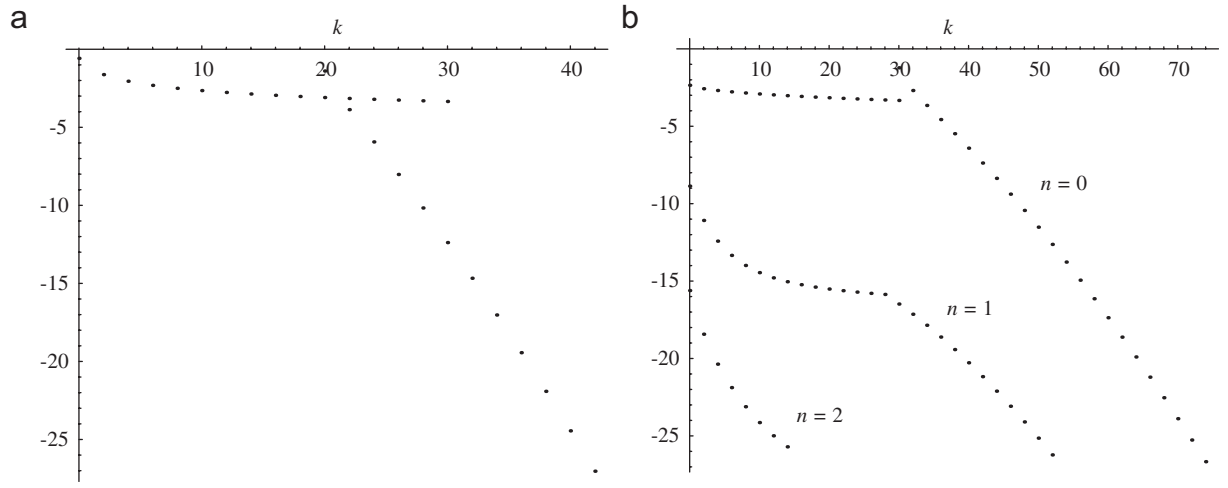

Fig. 5. The magnitude of the terms (on a $\log_{10}$ scale) as a function of ordinal number k when $a = 10^{-4}$ and $\theta = 0$: (a) the finite main sum and tail of I_1 and (b) the finite main sums at levels $n = 0, 1, 2$ with their modified tails (for $n = 0, 1$) of I_2.

Table 1
Absolute values of the error in $I(z; a)$ for different values of θ in the range $|\theta| \leqslant \frac{1}{2}\pi$ when the parameter $a = 10^{-4}$

θ/π	|Error|
0	3.494×10^{-25}
0.05	3.484×10^{-25}
0.10	3.706×10^{-25}
0.15	3.840×10^{-25}
0.20	4.618×10^{-25}
0.25	4.939×10^{-25}
0.50	1.671×10^{-24}
−0.05	3.740×10^{-25}
−0.10	3.928×10^{-25}
−0.15	4.746×10^{-25}
−0.20	5.265×10^{-25}
−0.25	7.031×10^{-25}
−0.50	3.056×10^{-24}

The Stokes line is $\theta = 0$. The truncation indices employed are indicated in the text.

For the integral I_1, which consists of only a single Hadamard series, we employed the truncation indices $(M_0, N_0) = (20, 20)$. For the integral I_2, we consider only the first three levels $0 \leqslant n \leqslant 2$ in (3.5), with $(M_0, N_0) = (30, 40)$, $(M_1, N_1) = (30, 20)$ and $(M_2, N_2) = (10, 0)$ (that is, no terms in the tail at level $n = 2$ are used). The absolute values of the terms in the expansions (3.3) and (3.5) against ordinal number are displayed in Fig. 5, where it can be seen that, with the above choice of truncation indices, the modified tails at each level decay at approximately the same rate as the initial asymptotic-like phase. The results of our computations are summarised in Tables 1 and 2 in which we present the absolute value of the error in $I(z; a)$ for different values of θ and $a > 0$. The exact value of $I(z; a)$ was obtained by numerical quadrature using *Mathematica* taking the path of integration to be the ray $\arg t = \frac{1}{2}\pi - \frac{1}{4}\theta$. It is seen that the accuracy level (*with fixed truncation indices*) remains uniform both in θ across the Stokes line $\theta = 0$ and as the parameter $a \to 0+$. The uniformity in a is a consequence of neither zeroth-level Hadamard series in I_1 and I_2 involving coefficients that result from expansion about the coalescing saddle t_{s1}.

We emphasise that the expansion (3.5) for I_2 is valid provided the discs of convergence ω_n about the points t_n $(n \geqslant 1)$ are controlled by the saddle t_{s1}, and not by the saddles t_{s2} or $t = 0$. We show below that this will be the case when (at least) $|\theta| \leqslant \frac{1}{2}\pi$. For θ in the ranges $\frac{1}{2}\pi < |\theta| < \pi$, the steepest descent path through t_{s1} becomes progressively more

Table 2
Absolute values of the error in $I(z;a)$ for different values of the parameter a as a function of θ

θ/π	|Error|			
	$a=10^{-2}$	$a=10^{-4}$	$a=10^{-6}$	$a=0$
0	3.813×10^{-25}	3.494×10^{-25}	3.491×10^{-25}	3.491×10^{-25}
0.05	3.798×10^{-25}	3.484×10^{-25}	3.481×10^{-25}	3.481×10^{-25}
0.10	3.964×10^{-25}	3.706×10^{-25}	3.704×10^{-25}	3.704×10^{-25}
0.15	4.217×10^{-25}	3.840×10^{-25}	3.835×10^{-25}	3.835×10^{-25}
0.20	4.803×10^{-25}	4.618×10^{-25}	4.617×10^{-25}	4.617×10^{-25}
0.25	5.411×10^{-25}	4.939×10^{-25}	4.933×10^{-25}	4.933×10^{-25}
	|Error|			
θ/π	$a=-10^{-1}$	$a=-10^{-2}$	$a=-10^{-4}$	$a=-10^{-6}$
0	4.840×10^{-25}	3.187×10^{-25}	3.502×10^{-25}	3.505×10^{-25}
0.05	7.326×10^{-25}	3.184×10^{-25}	3.491×10^{-25}	3.495×10^{-25}
0.10	7.752×10^{-25}	3.332×10^{-25}	3.634×10^{-25}	3.637×10^{-25}
0.15	8.619×10^{-25}	3.634×10^{-25}	3.938×10^{-25}	3.941×10^{-25}
0.20	1.440×10^{-24}	4.136×10^{-25}	4.437×10^{-25}	4.440×10^{-25}
0.25	1.331×10^{-24}	4.874×10^{-25}	5.173×10^{-25}	4.933×10^{-25}

The truncation indices employed are indicated in the text.

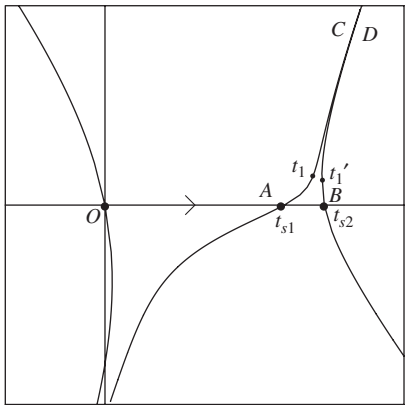

Fig. 6. The steepest descent paths through the saddle points for $0<a<1$ and $\phi_+(a)\leqslant\theta\leqslant\pi$ when the disc of convergence about the point t_1 on AC is controlled by the saddle t_{s2}. A possible integration path is the path $OABD$.

deformed in the neighbourhoods of t_{s2} and $t=0$ as $\theta\to\pm\pi$, eventually connecting up with these saddles when $\theta=\pm\pi$. The disc of convergence about the point t_1 on the upper half of the steepest descent path through t_{s1} when $\theta>0$ is specified by

$$\omega_0=\min\{|(\psi(t_1)-\psi(t_{s1}))\mathrm{e}^{\mathrm{i}\theta}|,\,|(\psi(t_1)-\psi(t_{s2}))\mathrm{e}^{\mathrm{i}\theta}|\}=\min\{\Omega_1,\,|\Omega_1+\mathrm{e}^{\mathrm{i}\theta}\Delta_+|\},$$

where $\Delta_+=\psi(t_{s1})-\psi(t_{s2})$. It follows that ω_0 is eventually controlled by the saddle t_{s2} when $\phi_+(a)\leqslant\theta\leqslant\pi$, where $\phi_+(a)=\arccos(-\Delta_+/(2\Omega_1))$. A similar argument when $\theta<0$ shows that ω_0 is controlled by the saddle at $t=0$ when $-\pi\leqslant\theta\leqslant\phi_-(a)$, where $\phi_-(a)=\arccos(-\Delta_-/(2\Omega_1))$ with $\Delta_-=\psi(t_{s1})-\psi(0)$. Since

$$\Delta_+=\tfrac{4}{3}a^{3/2},\quad \Delta_-=\tfrac{2}{3}a^{3/2}-\tfrac{1}{4}(a+1)^2+\tfrac{1}{3},$$

it is easily seen that $\Delta_\pm>0$ when $0<a<1$, and hence that $\phi_\pm(a)>\frac{1}{2}\pi$.

The situation when $\theta\geqslant\phi_+(a)$ is depicted in Fig. 6. Expansion about the point t_1 on the steepest descent path AC is now controlled by the second saddle in the cluster t_{s2}, so that the contribution from the path between t_{s1} and t_1 cannot

Table 3
Absolute values of the error in $I(z;a)$ for different values of θ in the range $|\theta|\leqslant\pi/4$ when the parameter $a=-10^{-1}$

θ/π	|Error|
0	4.840×10^{-25}
0.02	6.721×10^{-25}
0.04	7.665×10^{-25}
0.05	7.326×10^{-25}
0.06	6.576×10^{-25}
0.08	5.637×10^{-25}
0.10	7.752×10^{-24}
0.25	1.331×10^{-24}
−0.02	5.205×10^{-25}
−0.04	6.773×10^{-25}
−0.05	7.017×10^{-25}
−0.06	6.728×10^{-25}
−0.08	5.085×10^{-25}
−0.10	4.822×10^{-25}
−0.25	8.215×10^{-25}

The Stokes lines are given by $\pm\theta_c\doteq\pm0.0508\pi$. The truncation indices employed are indicated in the text.

be expressed as a *single* convergent Hadamard series. One way of overcoming this difficulty is to take as integration path the line segment connecting O with t_{s2} and thence along the neighbouring steepest descent path BD through t_{s2}. The disc of convergence about the point t_1' on BD is controlled by t_{s2}, so that the contribution from the path between t_{s2} and t_1' can now be expressed as a single convergent Hadamard series. The modified integration path is then the path $OABD$, with the inter-saddle contribution from AB being evaluated as a single Hadamard series similar to that resulting from the path OA.

3.2. The case $a<0$

When $a<0$, the saddle points t_{s1} and t_{s2} become a complex conjugate pair and typical steepest descent paths through the origin for $-a_*<a<0$ and $\theta\leqslant\frac{1}{2}\pi$ are shown in Fig. 2(d)–(i). The steepest descent paths for values of a and θ not in these ranges are similar and are not shown, the main difference being that there is no longer a Stokes phenomenon on $\theta_c(a)$ and $\theta=\frac{1}{2}\pi$ for $a<-a_*$. The modified path for $a<0$ is illustrated in Fig. 4(b): this again consists of replacement of C by the segment $[0,t_{s1}]$ followed by the upper half of the steepest descent path through the saddle t_{s1}. We observe that this choice covers all the situations depicted in Fig. 2(d)–(i) when $-a_*<a<0$ with a single path decomposition. The only significant difference is that the line segment joining the origin to t_{s1} is no longer on the real axis, so that the interval $\omega_0=\psi(t_{s1})-\psi(0)$ appearing in I_1 is now complex. In addition, unlike the situation prevailing when $a>0$, the discs of convergence about the sequence of points $t_1,t_2,\ldots$ on the steepest descent path in the integral I_2 are controlled only by the saddle t_{s1} throughout the range $|\theta|\leqslant\pi$. The integral $I(z;a)$ is then given by (3.6), with I_1 and I_2 defined in (3.3) and (3.5) for values of θ in this wider sector. Numerical results for θ straddling the Stokes lines $\pm\theta_c$ and a small negative value of a are presented in Table 3 using the same values of the truncation indices as in Section 3.1.

4. An example involving a cluster of three saddles

Our second example is the function $I(x)\equiv I(x;a,\kappa)$ defined by the Fourier integral

$$I(x)=\int_C(1+t)^{-1/2}\mathrm{e}^{-\mathrm{i}x\psi(t)}\,\mathrm{d}t,\quad \psi(t)=\tfrac{1}{4}t^4-\tfrac{1}{3}\kappa at^3+a^2(\tfrac{1}{2}t^2-\kappa at),\tag{4.1}$$

where x will be taken to be a large positive variable. The exponential factor is associated with a cluster of three saddle points situated at $t_{s1}=\kappa a$ and $t_{sj}=\pm\mathrm{i}a$ $(j=2,3)$, respectively. We take a as the (real) coalescence parameter and $\kappa\geqslant0$ is a parameter that alters the shape of the cluster. Here, we are primarily interested in the limit $a\to0$ when the saddles coalesce to form a single third-order saddle at the origin. The amplitude function $f(t)=(1+t)^{-1/2}$ possesses a remote (as $a\to0$) branch-point singularity at $t=-1$.

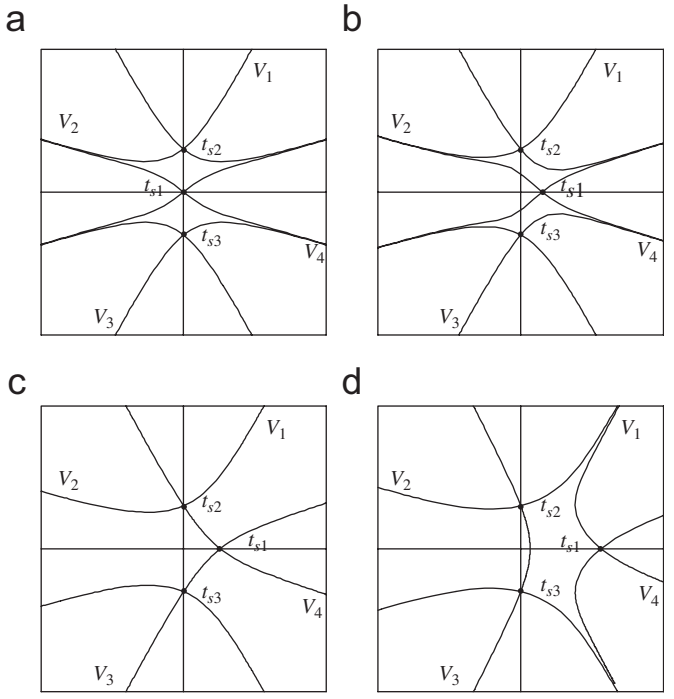

Fig. 7. The steepest descent and ascent paths when (a) $\kappa = 0$, (b) $0 < \kappa < \kappa_S$, (c) $\kappa = \kappa_S$ and (d) $\kappa > \kappa_S$. The saddles are denoted by heavy dots and labelled t_{sj} $(j = 1, 2, 3)$. The valleys (V) at infinity are indicated.

The exponential factor $\exp\{-\mathrm{i}x\psi(t)\}$ has valleys at infinity centred on the rays $\arg t = (4j-1)\pi/8$ $(j = 1, 2, 3, 4)$ which we label V_j. The paths of steepest descent and ascent through the saddles are displayed in Fig. 7 for different values of κ. For small κ, the saddles in the cluster are not connected by a common steepest descent path. As κ increases the saddles become connected when $\mathrm{Im}\{\mathrm{i}\psi(\pm\mathrm{i}a) - \mathrm{i}\psi(\kappa a)\} = 0$; that is, when $\kappa = \kappa_S$ where

$$\kappa_S = (2\sqrt{3} - 3)^{1/2} \doteq 0.68125.$$

For $\kappa > \kappa_S$, the saddle t_{s1} becomes is disconnected while the other two saddles t_{s2} and t_{s3} remain connected. To illustrate our procedure, we take the integration contour C in (4.1) to be a path connecting the valleys V_1 and V_3 at infinity. It is then easily seen that as κ increases through the value κ_S the number of contributing saddles changes by one, with the contribution from t_{s1} being switched off. This corresponds to a Stokes phenomenon which can occur for real variables; see the treatment of the Pearcey integral in [12,13].

As in the example in Section 3, we shall avoid decomposing the integration path C entirely into steepest descent paths. The paths from infinity leading to the saddles t_{s2} and t_{s3} will be chosen to coincide with the steepest descent paths through these saddles, but integration through the cluster will be along straight line segments. The actual choice of path through the cluster depends on the circle of convergence of the expansion (2.5) about t_{s2} or t_{s3}. For fixed a and sufficiently large κ, the saddle t_{s1} is more distant and consequently the disc of convergence about t_{s3} will be controlled by the neighbouring saddle t_{s2}, and vice versa. As κ decreases, the saddle t_{s1} steadily approaches the other two saddles with the consequence that ω_0 will eventually be controlled by t_{s1}. This happens when $|\psi(\mathrm{i}a) - \psi(-\mathrm{i}a)|$ and $|\psi(-\mathrm{i}a) - \psi(\kappa a)|$ are equal; that is, when

$$\tfrac{4}{3}\kappa a^4 = \tfrac{1}{12}a^4|(3 + \mathrm{i}\kappa)(\kappa + \mathrm{i})|.$$

The desired solution of this equation is given by $\kappa = \kappa_*$, where $\kappa_* = \sqrt{3}$. Thus, when $0 \leqslant \kappa < \kappa_*$, the disc of convergence about t_{s3} is controlled by t_{s1}, while when $\kappa > \kappa_*$ the disc of convergence is controlled by t_{s2}. Based on these considerations, we take as our paths of integration when $0 \leqslant \kappa \leqslant \kappa_*$ and $\kappa > \kappa_*$ those illustrated in Fig. 8. Since the

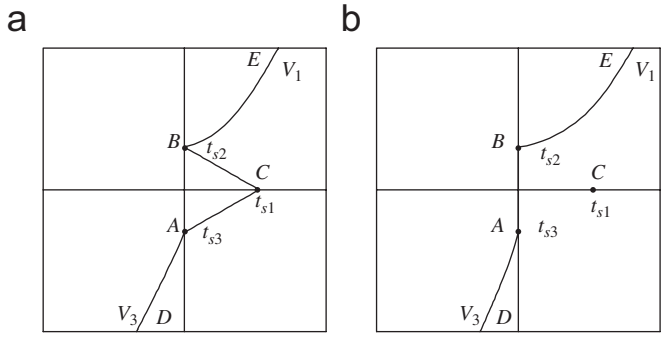

Fig. 8. The integration paths for (a) $0 \leqslant \kappa \leqslant \kappa_*$ and (b) $\kappa \geqslant \kappa_*$.

value of $\mathrm{Re}\{-\mathrm{i}\psi(t)\}$ at the saddles t_{sj} $(j = 1, 2, 3)$ is 0 and $\mp 2\kappa a^4/3$, respectively, it is seen that in both cases the integration path chosen progresses from a more dominant to a less dominant saddle.

We now consider the details of the Hadamard expansion for $I(x)$. When $\kappa \geqslant \kappa_*$, the integration path is the path $DABE$ shown in Fig. 8(b). From (2.6), the contribution I_{AB} from the path AB is given by

$$I_{AB} = \int_{t_{s3}}^{t_{s2}} (1+t)^{-1/2} \mathrm{e}^{-\mathrm{i}x\psi(t)}\,\mathrm{d}t = \mathrm{e}^{-\mathrm{i}x\psi(t_{s3})} \int_0^1 \mathrm{e}^{-x\omega_0 v}(1+t)^{-1/2}\frac{\mathrm{d}t}{\mathrm{d}v}\,\mathrm{d}v$$
$$= \mathrm{e}^{-\mathrm{i}x\psi(t_{s3})} \sum_{k=0}^{\infty} \frac{c_{k0}}{(\omega_0 x)^{(k+1)/2}} P(\tfrac{1}{2}k + \tfrac{1}{2}, \omega_0 x), \tag{4.2}$$

where

$$\omega_0 = \mathrm{i}\{\psi(t_{s2}) - \psi(t_{s3})\} = \tfrac{4}{3}\kappa a^4$$

and, from (2.5), the coefficients c_{k0} result from the expansion of $(1+t)^{-1/2}\,\mathrm{d}t/\mathrm{d}v$ about the saddle t_{s3}. The contributions from the steepest descent paths DA and BE are similar and are given by an expansion of the type (2.12), where the point t_1 on each path can be chosen independently of the coalescence parameter a. When $0 \leqslant \kappa \leqslant \kappa_*$, the integration path is the path $DACBE$ in Fig. 8(a); the procedure is similar except that the inter-cluster contribution I_{AB} is replaced by $I_{AC} + I_{CB}$. The contribution I_{AC} is given by (4.2) with $\omega_0 = \mathrm{i}\{\psi(t_{s1}) - \psi(t_{s3})\}$ and

$$I_{CB} = \mathrm{e}^{-\mathrm{i}x\psi(t_{s1})} \sum_{k=0}^{\infty} \frac{c'_{k0}}{(\omega'_0 x)^{(k+1)/2}} P(\tfrac{1}{2}k + \tfrac{1}{2}, \omega'_0 x),$$

where the quantity $\omega'_0 = \mathrm{i}\{\psi(t_{s2}) - \psi(t_{s1})\}$ and the coefficients c'_{k0} result from expansion of $(1+t)^{-1/2}\,\mathrm{d}t/\mathrm{d}v$ about the saddle t_{s1}.

In Fig. 9 we show the behaviour of the terms in the Hadamard expansion (4.2) of the contribution between the saddles t_{s3} and t_{s2} for a fixed value of a and different values of the parameter $\kappa \geqslant \kappa_*$. As κ decreases, the influence of the approaching saddle t_{s1} on the decay of these terms results in a series of oscillations which become progressively more pronounced as $\kappa \to \kappa_*$. When $\kappa = \kappa_*$, the convergence about t_{s3} is controlled by both t_{s1} and t_{s2}; for $\kappa < \kappa_*$, the disc of convergence about t_{s3} is controlled by t_{s1} and the terms in (4.2) then reach a global minimum before ultimately diverging.

The results of numerical calculations of $I(x)$ in (4.1) are presented in Table 4, where the absolute value of the error is displayed for $x = 15$ and different values of $a \to 0$. The exact value of $I(x)$ was obtained by numerical quadrature based on steepest descent paths. The truncation indices employed in the inter-cluster contributions (which consist of single Hadamard expansions) were $(M_0, N_0) = (20, 5)$, while those in the steepest descent contributions involved only the first two levels $0 \leqslant n \leqslant 2$ in (2.12) with $(M_0, N_0) = (30, 32)$, $(M_1, N_1) = (30, 15)$ and $(M_2, N_2) = (20, 0)$ (that is, no terms in the tail at level $n = 2$ are used). As in the example discussed in Section 3, the points t_n on the steepest descent paths through t_{s2} and t_{s3} are obtained from (2.9) and (2.10) with the value $\omega_0 = 0.75$. The level of

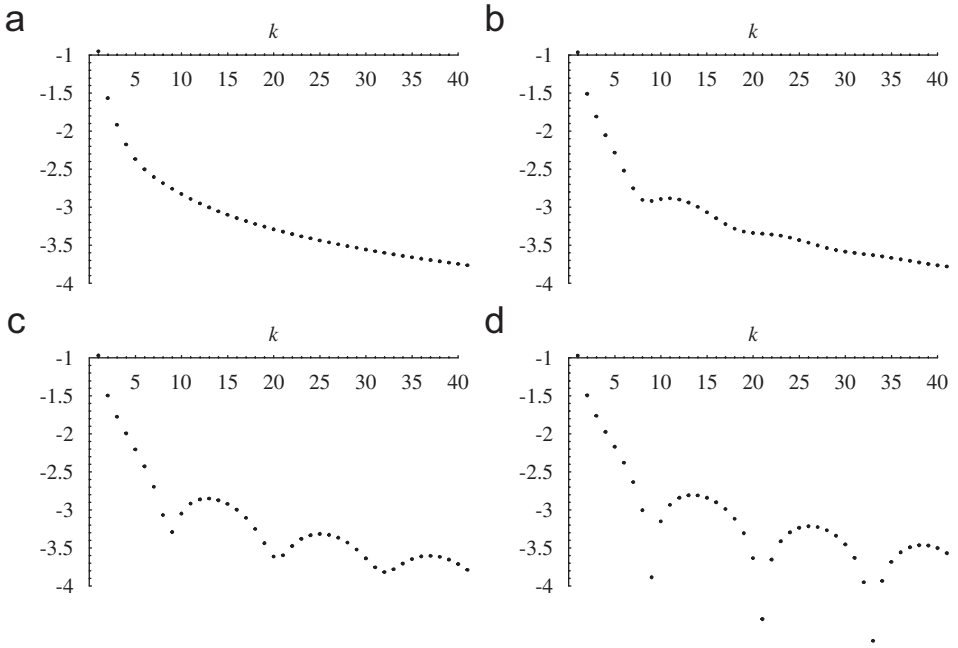

Fig. 9. The magnitude of the terms (on a $\log_{10}$ scale) of the inter-saddle series (4.2) as a function of ordinal number k and varying κ when $a = 0.1$ and $x = 15$: (a) $\kappa = 3.0$, (b) $\kappa = 2.0$, (c) $\kappa = 1.8$ and (d) $\kappa = \sqrt{3}$.

Table 4
Absolute values of the error in $I(x)$ for different values of a and κ when $x = 15$

κ	|Error|	
	$a = 0.1$	$a = 0.01$
0	1.051×10^{-21}	1.056×10^{-21}
0.5	1.034×10^{-21}	1.054×10^{-21}
κ_S	1.020×10^{-21}	1.053×10^{-21}
1.0	1.166×10^{-21}	1.051×10^{-21}
1.5	1.916×10^{-20}	1.049×10^{-21}
$\sqrt{3}$	9.983×10^{-22}	1.048×10^{-21}
2.0	9.922×10^{-22}	1.047×10^{-21}
3.0	9.750×10^{-22}	1.043×10^{-21}

accuracy of the computations (at fixed truncation indices) is uniform as both $a \to 0$ and as κ passes through the critical value κ_S (corresponding to a Stokes phenomenon). When $a = 0$, we have a single third-order saddle at the origin and the Hadamard expansion of $I(x)$ in this case could, of course, be evaluated by expansion about the origin as described in [8]. In this case, the result would consist of two expansions of type (2.8) in which $S_n(x)$ is given by (1.2) with $\alpha_0 = \beta_0 = \frac{1}{4}$. However, the expansion procedure described above will result in a uniform level of accuracy as $a \to 0$ since the zeroth-level Hadamard series employed do not involve coefficients related to the coalescing saddles.

5. A diffraction example

Our final example involves a cluster of three saddles which surrounds a fixed nucleus consisting of a double saddle point at the origin. In the treatment of the scattered wave field of the whispering-gallery mode at a point of local

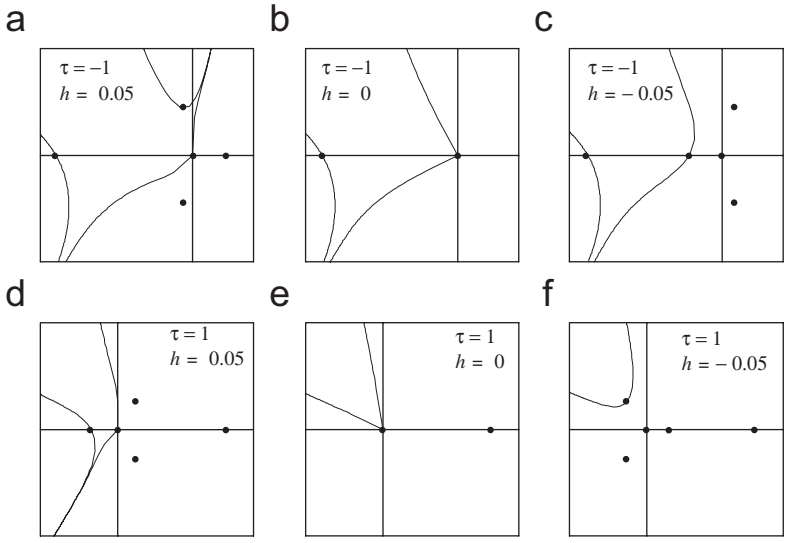

Fig. 10. Typical steepest descent paths for the solution (5.1) in the neighbourhood of the coalescence curve $h = \zeta - \frac{1}{2}\tau^4 = 0$. Only the relevant paths for the integration contour commencing and terminating at infinity in the sectors $(6\pi/7, \pi)$ and $(4\pi/7, 5\pi/7)$, respectively, are displayed. The saddles are denoted by heavy dots.

straightening of the boundary, it was shown in [5] that the wave field $\Psi(\zeta, \tau)$ satisfies the partial differential equation

$$\mathrm{i}\omega\frac{\partial\Psi}{\partial\tau} + \frac{\partial^2\Psi}{\partial\zeta^2} + 3\omega^2\tau^2\zeta\Psi = 0,$$

where ω is the wave frequency and ζ, τ are the spatial and time variables, respectively. The boundary conditions are that $\Psi(\zeta, \tau)$ decreases exponentially as $\zeta \to -\infty$ and behaves like an Airy function as $\tau \to -\infty$ (the incoming wave condition). The required solution is [5]

$$\Psi(\zeta, \tau) = \int_C \mathrm{e}^{\mathrm{i}\omega\psi(t)}\,\mathrm{d}t \tag{5.1}$$

with

$$\psi(t) \equiv \psi(t; \zeta, \tau) = \tfrac{9}{14}(t^7 - \tau^7) - (t^3 - \tau^3)(\zeta + \tfrac{1}{2}\tau^4 + \tau t^3)$$

and where the integration path C begins at infinity in the sector $(6\pi/7, \pi)$ and ends at infinity in the sector $(4\pi/7, 5\pi/7)$.

The exponential factor in (5.1) has, in general, six saddle points, some of which will move in the t-plane as the variables ζ and τ vary. The location of these saddles determines the asymptotic behaviour of $\Psi(\zeta, \tau)$ as $\omega \to +\infty$ in different domains of the ζ, τ-plane. Since

$$\frac{\partial\psi}{\partial t} = \tfrac{9}{2}t^2(t^3(t - \tfrac{4}{3}\tau) - \tfrac{2}{3}h), \quad h = \zeta - \tfrac{1}{2}\tau^4,$$

we see that the point $t = 0$ is a (fixed) double saddle with the other saddles given by the roots of the quartic equation $t^3(t - 4\tau/3) - 2h/3 = 0$. For small values of h, there is a remote saddle situated close to the point $t = 4\tau/3$ and a cluster of three saddles surrounding the double saddle given approximately by the roots of $t^3 = -h/(2\tau)$. When $h = 0$ (that is, on the curve $\zeta - \tau^4/2 = 0$ in the ζ, τ-plane), the saddles in the cluster coalesce with the double saddle at the origin to form a single fifth-order saddle, and the remote saddle is then situated at the point $t = 4\tau/3$. We shall be concerned here only with the situation corresponding to a neighbourhood of the coalescence curve $h = 0$; typical steepest descent paths for the integration contour C are illustrated in Fig. 10 for positive and negative τ. In Fig. 11 we show the number of contributory saddle points in different domains of the ζ, τ-plane. The change in the number of contributory saddles

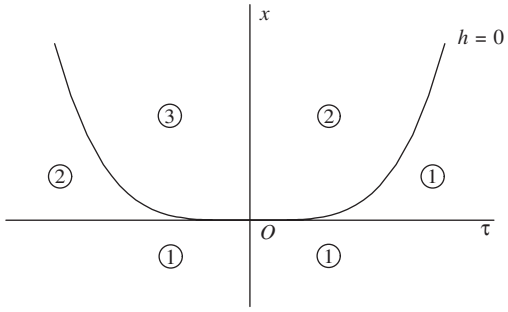

Fig. 11. The coalescence curve $h=\zeta-\frac{1}{2}\tau^4=0$ and the domains in the ζ, τ-plane corresponding to different numbers of contributory saddle points (shown encircled) for the integration contour C.

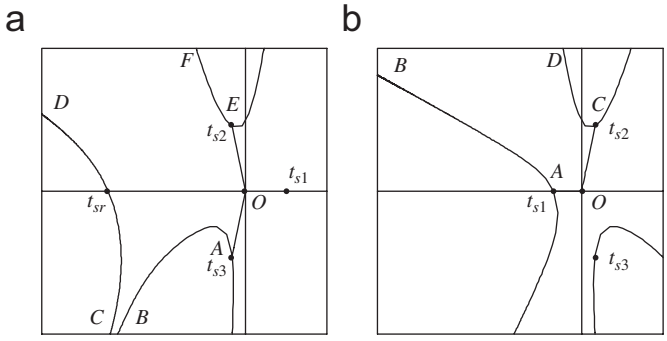

Fig. 12. The integration paths in the t-plane: (a) the path $DCBAOEF$ when $\tau=-1$, $h=0.05$ and (b) the path $BAOCD$ when $\tau=1$, $h=0.05$.

across the curve $h=\zeta-\frac{1}{2}\tau^4=0$ and the negative τ-axis is due to coalescence of saddles, while the change across the positive x-axis is due to a Stokes phenomenon. We do not discuss the last two effects any further here.

Inspection of Fig. 10 reveals that when $h<0$ (that is, below the coalescence curve) the integration path passes through only a single saddle in the cluster; above this curve, however, the integration path enters into the interior of the cluster. As the type of situation with $h<0$ has already been discussed in the previous examples, and the treatment of the case $h=0$ consisting of either one or two remote saddles is covered in [8], we concentrate on the case $h>0$ represented in Fig. 10(a), (d). To avoid problems of having discs of convergence on the steepest descent path through the origin being controlled by the complex saddles, we take the integration paths as shown in Fig. 12. The saddles in the cluster surrounding the fixed nucleus at the origin are labelled t_{sj} $(1\leqslant j\leqslant 3)$ and the remote saddle t_{sr} as indicated. In both cases, we follow steepest descent paths from the valleys at infinity, with the inter-cluster paths being straight line segments. As the two cases in the neighbourhood of the cluster are similar, we consider only the situation depicted in Fig. 12(b) in detail.

A straightforward computation shows that when $\tau=1$, $h=0.05$ the minimum value of $|\psi(0)-\psi(t_{sj})|$ $(1\leqslant j\leqslant 3)$ occurs when $j=1$, so that the disc of convergence about $t=0$ is controlled by the saddle t_{s1} indicated in Fig. 12(b). Consequently, to evaluate the contributions from the segments AO and OC we expand about the saddles t_{s1} and t_{s2}, respectively, rather than about $t=0$. Then, from (2.6), the Hadamard expansion of the contribution from the segment AO is given by

$$\mathrm{e}^{\mathrm{i}x\psi(t_{s1})}\sum_{k=0}^{\infty}\frac{c_{k0}}{(\omega_0 x)^{(k+1)/2}}P(\tfrac{1}{2}k+\tfrac{1}{2},\omega_0 x),$$

where for notational convenience we have set the wave frequency $\omega\equiv x$. The coefficients c_{k0} result from the expansion of type (2.5) about t_{s1} and $\omega_0=\mathrm{i}\{\psi(0)-\psi(t_{s1})\}$. The contribution from the steepest descent path BA leading to the saddle t_{s1} is given by an expansion of the type (2.12), where the point t_1 on the path can be chosen independently of

Table 5
Absolute values of the error in $\Psi(\zeta, \tau)$ for different values of $h \equiv \zeta - \frac{1}{2}\tau^4$ when $\tau = 1$ and $\omega = 15$

h	|Error|
0	9.674×10^{-20}
0.01	1.107×10^{-19}
0.02	1.282×10^{-19}
0.04	1.705×10^{-19}
0.05	2.122×10^{-19}
0.10	3.136×10^{-19}
−0.01	3.167×10^{-20}
−0.02	5.303×10^{-20}
−0.04	9.110×10^{-20}
−0.05	1.069×10^{-19}
−0.10	1.428×10^{-19}

The truncation indices employed are given in the text.

the coalescence parameter h (in the numerical computations we set $\omega_0 = 0.60$). Analogous expansions apply for the contributions from the path OC and the steepest descent path CD from the saddle t_{s2}.

The results of numerical computations with $\omega \equiv x = 15$ are presented in Table 5 for different values of h when $\tau = 1$. The exact value of $\Psi(\zeta, \tau)$ was obtained by numerical quadrature based on steepest descent paths. The truncation indices employed in the inter-cluster contributions when $h > 0$ (which consist of single Hadamard expansions) were $(M_0, N_0) = (10, 7)$, while those in the steepest descent contributions involved only the first two levels $0 \leqslant n \leqslant 2$ with $(M_0, N_0) = (25, 25)$, $(M_1, N_1) = (25, 15)$ and $(M_2, N_2) = (25, 0)$ (that is, no terms in the tail at level $n = 2$ are used). When $h \leqslant 0$, only the steepest descent paths through the relevant saddle (see Fig. 10(e), (f)) are employed in conjunction with an expansion of type (2.12) with $\omega_0 = 0.60$. It is seen that a uniform level of accuracy (at fixed truncation indices) can be maintained through coalescence of the cluster.

Acknowledgement

The author wishes to acknowledge helpful discussions with D. Kaminski.

References

[1] M.V. Berry, C.J. Howls, Hyperasymptotics for integrals with saddles, Proc. Roy. Soc. London A 434 (1991) 657–675.
[2] C. Chester, B. Friedman, F.J. Ursell, An extension of the method of steepest descents, Proc. Cambridge Philos. Soc. 53 (1957) 507–522.
[3] W. Gautschi, F.E. Harris, N.M. Temme, Expansions of the exponential integral in incomplete gamma functions, Appl. Math. Lett. 16 (2003) 1095–1099.
[4] C. Howls, P.J. Langman, A.B. Olde Daalhuis, On the higher-order Stokes phenomenon, Proc. Roy. Soc. London 460A (2004) 2285–2303.
[5] A.Ya. Kazakov, Special function related to the scattering of the whispering gallery mode at the point of local straightening, Zap. Nauchn. Sem. POMI 300 (2003) 180–186.
[6] C. Morosi, L. Pizzocchero, On the expansion of the Kummer function in terms of incomplete gamma functions, Arch. Inequality Appl. 2 (2004) 49–72.
[7] K.E. Muller, Computing the confluent hypergeometric function, Numer. Math. 90 (2001) 179–196.
[8] R.B. Paris, On the use of Hadamard expansions in hyperasymptotic evaluation of Laplace-type integrals: I. Real variable, J. Comput. Appl. Math. 167 (2004) 293–319.
[9] R.B. Paris, On the use of Hadamard expansions in hyperasymptotic evaluation of Laplace-type integrals: II. Complex variable, J. Comput. Appl. Math. 167 (2004) 321–343.
[10] R.B. Paris, Exactification of the method of steepest descents: the Bessel functions of large order and argument, Proc. Roy. Soc. London A 460 (2004) 2737–2759.
[11] R.B. Paris, D. Kaminski, Asymptotics and Mellin–Barnes Integrals, Cambridge University Press, Cambridge, 2001.
[12] R.B. Paris, D. Kaminski, Hyperasymptotic evaluation of the Pearcey integral via Hadamard expansions, J. Comput. Appl. Math. 190 (2006) 437–452.
[13] F.J. Wright, The Stokes set of the cusp diffraction catastrophe, J. Phys. A 13 (1980) 2913–2928.